6
Bibliografia

ASSOCIAÇÃO BRASILEIRA DE NORMAS TÉCNICAS. ABNT 6152: **Materiais metálicos – Ensaio de Tração à Temperatura Ambiente,** MAIO 2002.

ACH, R.S., CASTRO NETO, J., NOBREGA, M.J.R., CASTRO, J.T.P., SPERANZA NETO, M. **Influencia da Taxa de Deformação nas Curvas Tensão Deformação de um Aço 1020 Pré Encruado**. 65º Congresso Anual ABM, 2010.

ASM HANDBOOK. **Mechanical Testing and Evaluation,** Vol 8, p 245-249, ASM International, 2000.

ASME B 31.8. **Gas Transportation and Distribution Piping Systems** , 2003.

_____. 31.4. **Pipeline Transportation Systems for Liquid Hydrocarbons and Others Liquid*s***, 2006.

BACKOFEN, W.A**. Deformation Processing**, Addison-Wesley, 1972.

BOX, G. E. P., HUNTER, **Statistics for Experimenters: Design, Innovation, and Discovery,** 2nd Edition, 2005.

BOYCE, B.L., CRRENSHAW, T.B., DILMORE, M.F.**The Strain-Rate Sensitivity of High-Strength High-Toughness Steels.** Sandia National Laboratories, 2007.

BRUCE, D. **Dynamic tensile testing of sheet steels and influence of strain rate on strengthening mechanisms in sheet steels**, Ph.D. Thesis, Colorado School of Mines, 2003.

CASTRO, J.T.P.; MEGGIOLARO, M.A. **Fadiga - Técnicas e Práticas de Dimensionamento Estrutural sob Cargas Reais de Serviço**: Volume II - Propagação de Trincas, Efeitos Térmicos e Estocásticos", ISBN 1449514707, CreateSpace, 2009.

CHEN, Y., CRAIG, C., TYAN, T., LAYA, J. and CHENG, J. **Finite Element Modeling of the Frame for Body on Frame Vehicles: Part II-Full Vehicle Crash.**SAE International, 2004.

COTTRELL, A.H. **The Mechanical Properties of Matter**, Krieger, 1981.

DIETENBERGER, M., BUYUK, M., KAN, CD. **Development of High Rate Dependent Vehicle Model**.University of Stuttgard, Stuttgard, Germany, 2005.

DIETER , G.E., **Mechanical Metallurgy**, McGraw Hill, 1976.

FROST, H.J.; ASHBY, M.F. **Deformation Mechanisms Maps**, Pergamon, 1982.

HERTZBERG, R.W. **Deformation and Fracture Mecahncis of Engineering Materials**, 3rd Edition, John Wiley & Sons, New York, 1989.

HUANG, G., ZHU, H. **The Effect of Strain Rate on Tensile Properties and Fracture Strain**, ArcelorMittal, USA, 2007.

KHARCHENKO, V.V. **Viscoplastic Model in Simulation Viscoplastic Model in Simulation of High Strain-Rate Behavior of Materials.** Strength of Materials, Vol. 34, No. 3, 2002.

LAROUR, P. **Strain Rate Sensitivity of Automotive Sheet Steels: Influence of Plastic Strain, Strain Rate, Temperature, Microstructure, Bake Hardening and Pre- Strain**. Villeneuve la Garenne, Paris, 2010.

LEMAITRE, J.; CHABOCHE, J.L. **Mechanique des Matériaux Solides**, Bordas, 1985.

MATIAS, J. L. H. **Técnicas de Penalidade e Barreira Baseadas em Métodos de Pesquisa Direta e a Ferramenta PNL-Pesdir**, Tese de Doutoramento, UTAD, 2003.

MEYERS, M.A., **Mechanics and Materials**, John Wiley & Sons, 1999.

MILITSKY, M. **Effects of pre-strain on the mecahncial properties of low-carbon steels tested over a wide range of strain rates**, M.S. Thesis, Colorado School of Mines, 2000.

NATIONAL INSTITUTE OF STANDARDS TECNOLOGY, **Mechanical Properties of Structural Steels**, 2005.

NEMAT-NASSER, S., GUO, WG. **Experimental Investigation of Energy-Absorption Characteristics of Components of Sandwich Structures,** Center of Excellence for Advanced Materials, Department of Mechanical and Aerospace Engineering, University of California, USA, 2006.

NOBREGA, M.J. **Influência da Metodologia de Medição das Propriedades Mecânicas Dinâmicas na Previsibilidade do Comportamento de Estruturas Sujeitas a Impactos Elastoplásticos.** Tese de Doutorado, PUC RJ, 2010.

PEIXINHO, N., DOELLINGER, C. **Characterization of Dynamic Material Properties of Light Alloys for Crashworthiness Applications,** Departamento de Engenharia Mecânica, University of Minho, Portugal, 2010.

SHOROT, A., BAKER, M. I**s It Possible to Identify Johnson-Cook Law Parameters from Machining Simulations,** Technische Universität Braunschweig, Institut für Werkstoffe, Germany, 2010.

SILVA, L.R.O. **Ensaio de Tração a Temperatura Ambiente:Diretrizes para Implementação da Incerteza de Medição**. ENQUALAB, 2004.

SOUZA, S.A. **Ensaios Mecânicos de Materiais Metálicos.** 4ºed., São Paulo,Edgard Blucher Ltda, 1974.

TAKAGI, S., OGAWA, K., MIMURA, K., TANIMURA, S. **Stress-Strain Curves of High Strength Steel Sheets at Strain Rates from 10^{-3} s^{-1} to $10^{3}s^{-1}$ Obtained with Various Types of Tensile Testing Machines.** Journal of Material and Manufacturing, Vol.114, nº5, p.166-174, 2005.

THOMPSON, A.C. **High Strain Rate Characterization of Advanced High Strength Steels,** Waterloo, Ontario, Canada, 2006.

XIAO, X. **Dynamic Tensile Testing of Plastic Materials.** General Motors Corporation, Elsevier, p.1- 4, 2007.

ZABOTKIN, K., O´TOOLE, B., TRABIA, M. **Identification of the Dynamic Tensile Properties of Metals under Moderate Strain Rate.** 16th ASCE Engineering Mechanics Conference, University of Washington, Seattle, 2003.

APÊNDICE A
Artigo Técnico Apresentado na 65º Congresso da ABM – Internacional

STRAIN RATE INFLUENCE ON THE STRESS-STRAIN BEHAVIOR OF A COLD WORKED 1020 STEEL [1]

Rafael Salomão Ach [2]
Jaime de Castro Neto[3]
Marcelo de Jesus Rodrigues da Nóbrega[4]
Jaime Tupiassú Pinho de Castro[5]
Mauro Speranza Neto[5]

Abstract

Stress×strain $\sigma \times \varepsilon$ curves of a cold worked 1020 steel were measured controlling the strain-rate imposed on the test specimens (and not the testing machine piston or load bean speed), in the range $10^{-5} \leq \dot{\varepsilon} \leq 3\ s^{-1}$. This ample data set, properly treated by a versatile software developed to acquire, filter and present the data in real time, was used to verify the adequacy of several models proposed to describe the strain-rate influence, using an Levenberg-Marquardt optimization algorithm to fit the models to the ensemble of the measured data. This relatively simple procedure avoids the intrinsic systematic errors associated to the traditional practice of measuring the strain-rate effect on the $\sigma \times \varepsilon$ curves controlling the load speed, which may be particularly relevant when testing steel specimens, as their stiffness is many times at least an order of magnitude greater than those of the testing machines.

Key words: strain-rate effects, dynamic mechanical behavior, optimal data fitting.

---

[1] *65º Congresso da ABM - Internacional. 26 a 30 de julho de 2010. Rio de Janeiro - RJ - Brasil.*
[2] *Engenheiro Mecânico, mestrando PUC-Rio.*
[3] *Estagiário, Tecgraf PUC-Rio.*
[4] *Mestre, professor CEFET/RJ, doutorando DEM PUC-Rio.*
[5] *Doutor, professor DEM PUC-Rio.*

1 INTRODUCTION

The influence of strain rate $\dot{\varepsilon}$ in Stress x strain curves, in general neglected in the design of mechanical structural metallic, it may be important in practice. The dynamic effect on the mechanical properties may be relevant in parts working under high stress generated by loads much slower or faster than usual in the tensile testing used to measure them (lasting 1-2 minutes, typical average rates on the order of $\dot{\varepsilon} \cong 2.5 \cdot 10^{-3}\ s^{-1}$). For example, as loads very slow are generally associated with the lowest resistance, damage around defects or cracks in the test overloading pipe can be much larger than those provided for ignoring the effect of rate. Moreover, the simulation of automotive accidents can only be made using well elastoplastic mechanical properties obtained from curves **(σ×ε)** measured under rates quite high, similar to the real accident.

Several mechanisms may cause deformation rate effects on mechanical properties, generated by dissipative nature of plastic deformation [(1)]. However, your description is not part of this work, which refers only to assess the adequacy of phenomenological models used to quantify them in dimensional mechanical [(2-6)]. These models do not reflect the physical complexity of the problem, but still have great practical importance. In fact, its uncertainty, which depends on several factors, which often limits the quality of structural predictions. Among them, the practice of adjusting the parameters of the models to measured data in tensile tests made at rates of loading or constant displacement, rather than under fixed strain rates.

This inadequate practice is widely used because facilitates the tests (it is trivial to set, eg, the speed of the beam in a testing machine operated by screws). But this procedure certainly does not guarantee a constant strain rate in the specimen (CP) and prediction errors can cause very significant.

The load applied on the tensile test requested both the CP and the structure of -machine testing, which, despite working elastically, may undergo significant displacement. In fact, CP steel 10 mm in diameter are an order of magnitude stiffer than the machines used to test them, whose rigidity is typical 7 <K <32 MN/m [(3)] Thus, the strain rate of CP on test controlled by the speed **v** of the load is obtained as:

$$\mathbf{vt} = \frac{\mathbf{P}}{\mathbf{K}} + \frac{\sigma \mathbf{L}}{\mathbf{E}} + \varepsilon_{\mathbf{p}} \mathbf{L} \Rightarrow \dot{\varepsilon} = \frac{(\mathbf{vK}/\mathbf{AE}) + \dot{\varepsilon}_{\mathbf{p}}}{(\mathbf{KL}/\mathbf{AE}) + \mathbf{1}} \tag{1}$$

where **t** is the testing time, **σ** is the stress acting on the CP, **L** its length, **A** the area of section resistant, **E** modulus of elasticity, $\dot{\varepsilon}$ the strain rate, ε_p plastic strain acting on it; and **P** is the applied load.Therefore, even assuming that the machine has a stiffness constant (which generally does not occur due to the nonlinear behavior of claws and joints), strain rate acting on the CP **is not** proportional to the velocity of the load applied on it. Except in the elastic region (in which dynamic effects are negligible), when equation (1) is summarized to

$$\dot{\varepsilon}_e = \frac{v}{L}\left(1 + \frac{AE}{KL}\right) \tag{2}$$

However, the constitutive relations to quantify dynamics effects in the region of curves **(σ×ε)** elastoplastic (a fixed temperature) are of the form **σ = f (ε, $\dot{\varepsilon}$)** as shown, eg, by Johnson-Cook popular model[2-3] which, given a fixed temperature, uniaxial in this case, can be given by:

$$\sigma = S_{E_0} \cdot \left[1 + B \cdot (\varepsilon - \varepsilon_E)^n\right] \cdot \left[1 + C \cdot \ln(\dot{\varepsilon}/\dot{\varepsilon}_0)\right] \tag{3}$$

where ε and σ are the strain and stress acting on CP traction after its disposal; S_{E0} is the yield strength as a reference rate $\dot{\varepsilon}_0$; $\varepsilon_E = S_E/E + 0.002$ is the deformation associated to the yield strength, E is the modulus of elasticity, B and n are parameters to quantify the hardening (static) of material, and C is the parameter that quantifies the effect (supposed log) of the shear rate curves (σ×ε) material. This is the proper way to write the equation of Johnson-Cook (for $\sigma = S_{E0}$ if $\varepsilon = \varepsilon_{E0}$ e $\dot{\varepsilon} = \dot{\varepsilon}_0$), which in principle should be applied to real stresses and strains, but is also used to describe the effect of the rate stress and strain engineering

There are several other similar semi-empirical models which purports to describe the effect of the strain rate at curves **(σ×ε)** dynamically measures [1-6]. However, measuring the various parameters of these models is often made from tensile tests performed under the control of speed, **assuming** that the strain rate is given by $\dot{\varepsilon} = v/L$ a procedure definitely unsuitable even in the elastic region, as seen above. To illustrate this problem, CPs steel of 9 mm diameter were tested in a servo-hydraulic machine in two control strategies, see Fig 1 [7]: (i) fixed shear rate, using a clip gage mounted to the CP measuring its deformation, and (ii) speed of the fixed piston, controlling the movement of the piston through the LVDT mounted thereon. From the input data of the program used, the command signal is compared to the feedback signal, thereby generating an error signal that is used to actuate the servo-valve controlling the flow of hydraulic fluid to the actuator. The control signal can be generated by the clip mounted on the gage or the CP LVDT set between the piston and the machine frame.

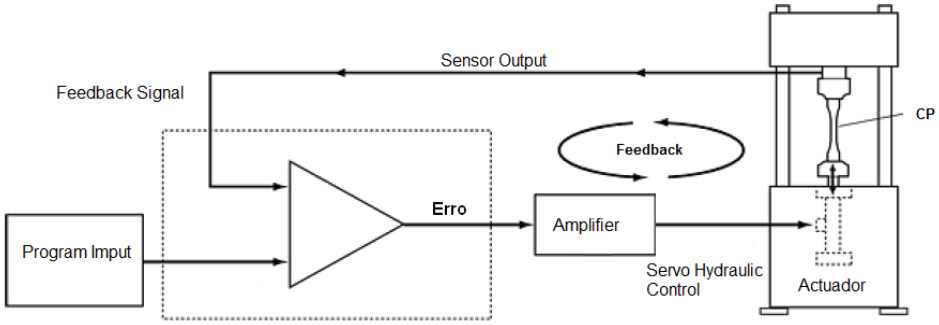

Figure 1. Basic diagram of the control system of a servo-hydraulic machine.

Figure 2 shows the displacement of the piston and the strain imposed on CP during a test under control of the strain rate, fixed and equal to 5 x 10^{-2} %/s during the test. It is noted here that the speed of the piston would generate an estimated variable for the test, whose mean given by $\dot{\varepsilon} = v/L = 9.6 \cdot 10^{-2}$%/s has a value much higher than the measured rate.

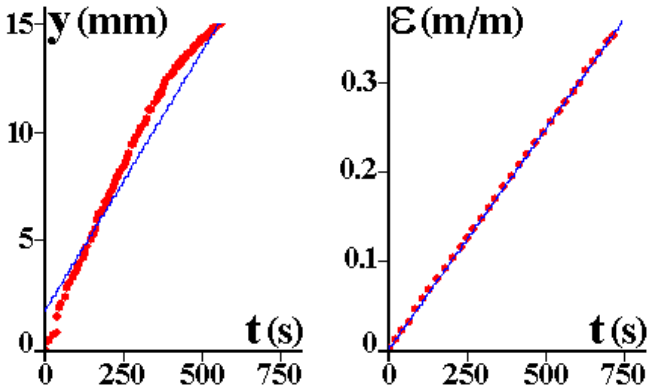

Figure 2. Piston displacement x engineering strain active in the CP during a test performed under constant strain rate

Figure 3 shows the measurements of piston displacement and strain resulting in the CP identical to Figure 2 during a test run under the control of velocity of the piston, held fixed. In this case the speed was adjusted to generate a deformation rate of CP estimated by $\dot{\varepsilon} = v/L = 4.8 \cdot 10^{-2}$%/s, almost equal to the rate imposed in the previous test. However, the average strain rate of CP was actually measured at much lower, $\dot{\varepsilon}_m = 3 \cdot 10^{-2}$%/s, ranging from $\dot{\varepsilon} \cong 2.2 \cdot 10^{-2}$%/s at the beginning to about $4.5.10^{-2}$%/s at the end of test.

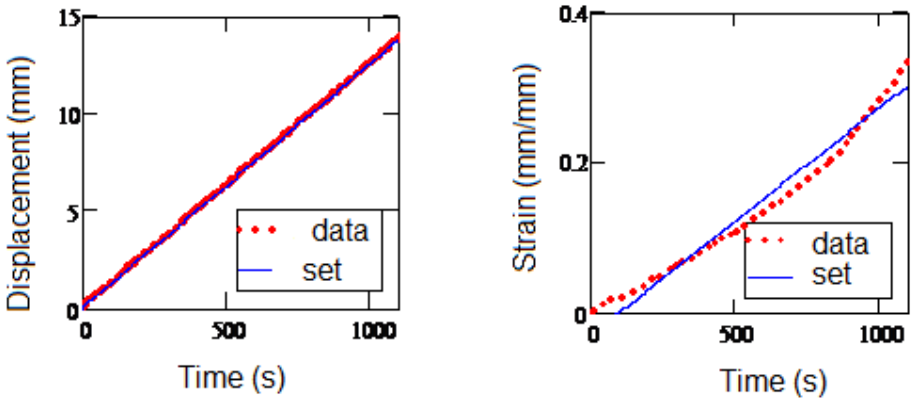

Figure 3. Piston displacement x engineering strain active in the CP equal to figure 2, for a test carried out under fixed piston velocity.

These differences are not insignificant, and can significantly affect the uncertainty of test results. However, this limitation does not affect any of those discussed here, all measured under constant rate. Then, is made a brief description of the experimental system and the program acquisition and data processing **(σ×ε)** dynamic, and presents a set of 13 curves measured under $10^{-5} \leq \dot{\varepsilon} \leq 3\ s^{-1}$ (in tests which lasted for about 3 hours to less than 50 ms). Hereafter, are described 3 phenomenological models studied here, Johnson-Cook, Zerilli-Armstrong [6], and a modified Johnson-Cook. After the model parameters are adjusted to the set of experimental data using an optimization algorithm Levenberg-Marquardt [8]. Finally, to evaluate the accuracy of the various models and presenting any suggestions to generalize and standardize this test procedure.

2 MATERIAL AND PROCEDURES

The material tested was a 1020 steel for cold-rolled with the yield strength and tensile strength (measured at the usual rate $\dot{\varepsilon} = 2.5 \cdot 10^{-3}\ s^{-1}$) $\mathbf{S_E}$ = 589 and $\mathbf{S_R}$ = 651 MPa. The tests described below were performed under control of strain rate in a servo-hydraulic machine computed Instron 8501 of 100 kN, having a Moog servo 40 l / min, using a transducer strain gage Instron clip-20 260-604 as base mm and 12.5 mm strip trative and hydraulic clutches carefully aligned within 0.01 mm. The CPs of 10 mm diameter were machined according to ABNT 6152

The lowest strain rate used in the tests was limited by mechanical noise intrinsic to the servo and the signal / noise ratio of the transducer, while the highest was restricted by the flow capacity of the servo and the speed of digital control system of the machine, whose rate acquisition is 5 kHz. Despite the conventional tensile tests is very simple, measure curves **(σ×ε)** operating within the limits of the test machines is not an elementary task properly. It is worth emphasizing that these limits depend very much on details that are not obvious such as: the quality of the electrical grounding, alignment, clearances and stiffness of the clutches and other components of the freight train, and the rigidity of the assembly clip-gage in the CP

(which control the natural frequency response and its dynamics), and the rate of acquisition and gains of the feedback loop PID control of the machine. The setting of this last detail, in particular, requires experience and skill of the operator of the machine, and some familiarity with the basic concepts of control theory.

The data acquisition system developed for this work consists of capture AD board and two programs, written in Labview language. The board reads and digitizes the signals from the clip gage and load cell and sends them to the first program, which is a plot of real-time data measured during the test, see Figure 4, and stores them in an appropriate file. The second program is the analysis of such data and filtering to remove noise reading, generating curves $(\sigma \times \varepsilon)$ engineering and real as those shown below.

The first model studied here, which describes the effect on the rate curves elastoplastic is the Johnson-Cook, described above. The second is the modified Zerilli-Armstrong [6], using the notation of eq. (3) on a fixed temperature is given by:

$$\sigma = S_{E_0} + B_1 \cdot (\varepsilon - \varepsilon_E)^n + C_1 \cdot \exp\left(1.5 \cdot \dot{\varepsilon}/\dot{\varepsilon}_0\right) \tag{4}$$

Also studied was a variation of the model given by Johnson-Cook given by:

$$\sigma = S_{E_0} \cdot \left[1 + B \cdot (\varepsilon - \varepsilon_E)^n\right] \cdot \left[1 + C \cdot \ln\left(\dot{\varepsilon}/\dot{\varepsilon}_0\right)\right]^{1.4} \tag{5}$$

The model parameters must be adjusted to describe the set of all the experimental points measured in the various tests, not just the curves measured in each test. This task can be executed by the algorithm Levemberg-Marquardt (LM), which minimizes the square error between the predictions generated by nonlinear models and the experimental points, just allows you to evaluate the quality of the models studied. In mathematical terms, **m** data points (x_i, y_i), $i = 1, \cdots, m$, LM iteratively seeks the vector $p = [p_1, p_2, \cdots, p_n]^T$ (where **T** means transpose) of n adjustable parameters of the model f (x, p) specified so that they minimize the sum **S (p)** of the quadratic deviations between the different measured values y_i and calculated values in points x_i (using the different set parameters p_j of the function **f**):

$$S(p) = \sum_{i=1}^{m} \left[y_i - f(x_i, p)\right]^2 \tag{6}$$

Some generic programs such as Mathcad eg, have dedicated functions that perform these calculations (whose convergence, say by the way, is very sensitive to initial guess values of the unknowns). For details, see [8].

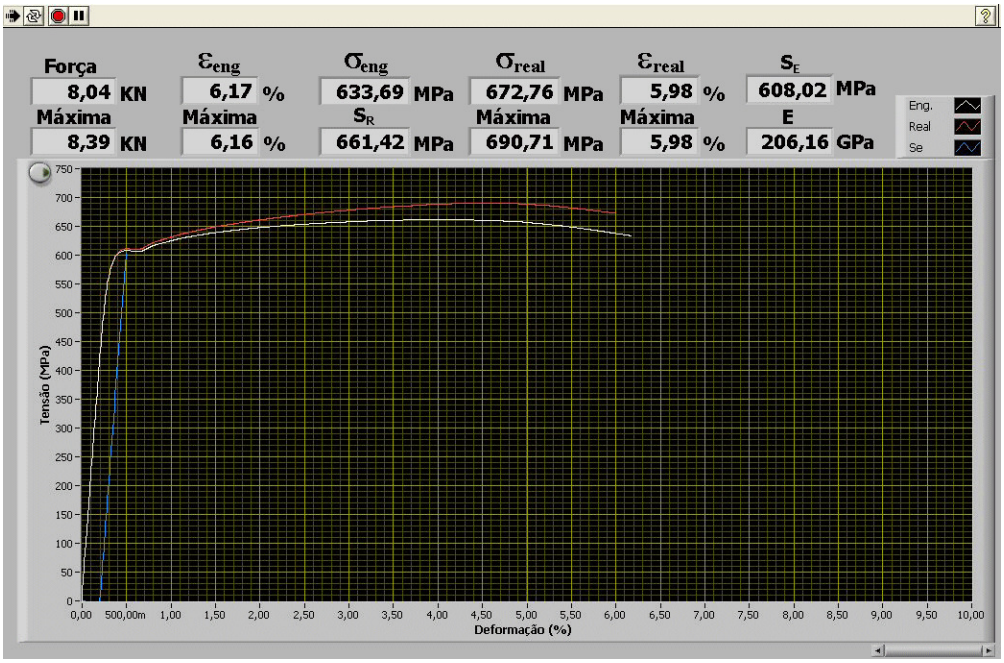

Figure 4. Screen monitoring of tensile tests in real time.

3 EXPERIMENTALS RESULTS AND ANALYSIS OF THE MODEL

The yield strength (S_E) and tensile strength (S_R) measured during the tests at various strain rates imposed in the CPs are listed in Table 1. Engineering curves in these tests are shown in Figure 5, and the real curves until necking are shown in Figure 6. Table and Figures show the sensitivity of the 1020 steel tested under strain rate, which in these tests ranged from 5 ½ orders of magnitude, causing a range of about 10% between the lower and higher strength at plastic strain measured.

So, ranging $\dot{\varepsilon}$ from $\mathbf{10^{-5}}$ to **3/s**, strengths increase (S_E) and (S_R) of about 10% which is easily identifiable in the graphs, but not too large. Therefore, this material could be used in ignoring sized pieces, as usual, the effect of loading rate, provided that safety factors using the marketing 'typical', $\phi_E = S_E/\sigma_{max} > 1.25$ (with S_E as the rate "normal" $\dot{\varepsilon} \cong 0.25\%/s$). However, these data indicate that the effect of rate should not be ignored when dimensioning have very high stress, the order of SE or greater, as in the examples mentioned in the introduction. It is worth mentioning that Figure 5 shows that higher rates are almost always associated with ductility greater than measured at lower rates, a fact not intuitive.

	Engineering Curve		Real curve	
$\dot{\varepsilon}$ (s^{-1})	S_E (MPa)	S_R (MPa)	S_E (MPa)	S_R (MPa)
10^{-5}	578	636	581	655
10^{-4}	583	647	588	673
10^{-4}	583	648	585	668
$2.5 \cdot 10^{-3}$	589	651	591	679
0.01	599	662	602	691
0.01	606	673	609	705
0.01	606	675	610	709
0.1	610	675	613	706
0.1	620	684	623	716
0.1	623	683	626	711
1	620	693	624	741
1	621	691	624	730
3	628	696	631	734

Tabela 1. yield strength (SE) and tensile strength (SR) as a function of $\dot{\varepsilon}$

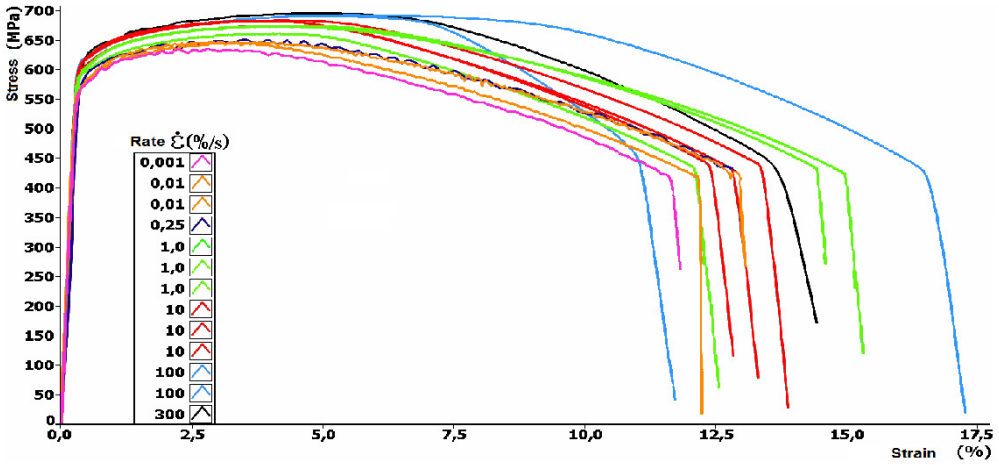

Figure 5: The 13 curves σ×ε engineering measures in the various rates tested

The intrinsic dispersion of the tests can be assessed by comparing the curves measures at equal rates. Repeated trials with the same strain rate, the dispersion was increased to a rate of 1.0% / s, but well below 2.0% suggested by ABNT 6152. This confirms the quality of the experimental system used, and ownership of the variation observed between the curves measured at various rates tested. In response, the adjustment of mathematical models to experimental curves were performed using only one of the curves measured at rates 10^{-5}, 10^{-4}, 10^{-3}, 10^{-2}, 0.1, 1 and 3/s, not to hinder the their graphical comparison.

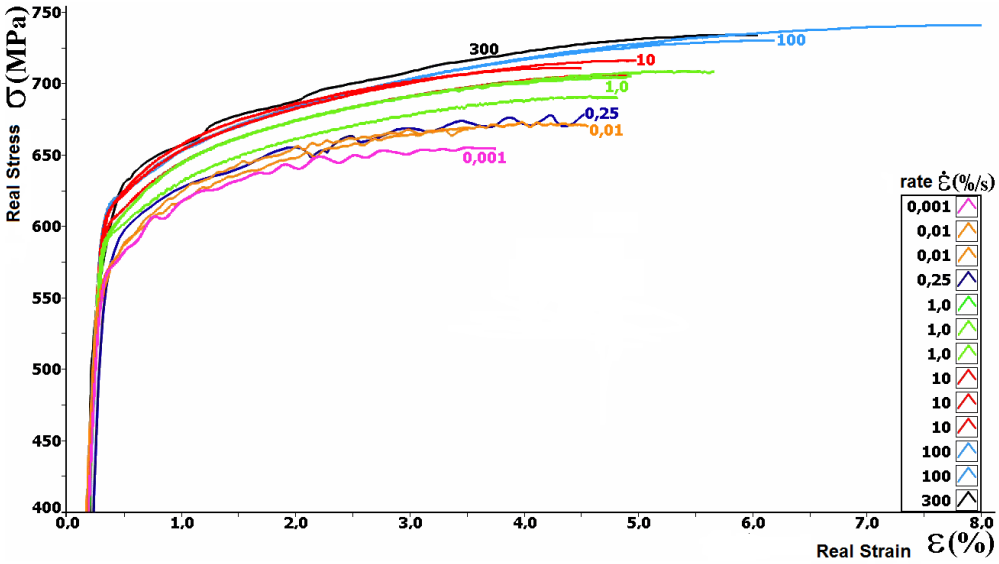

Figure 6: Detail of the plastic region of stress strain real curves (to necking) calculated from the data in Figure 5.

Figs 7-9 show the adjustment by LM in Johnson Cook-in-Zerilli Armstrong and the modified Johnson-Cook to the curves (**σ×ε**) real measurements.

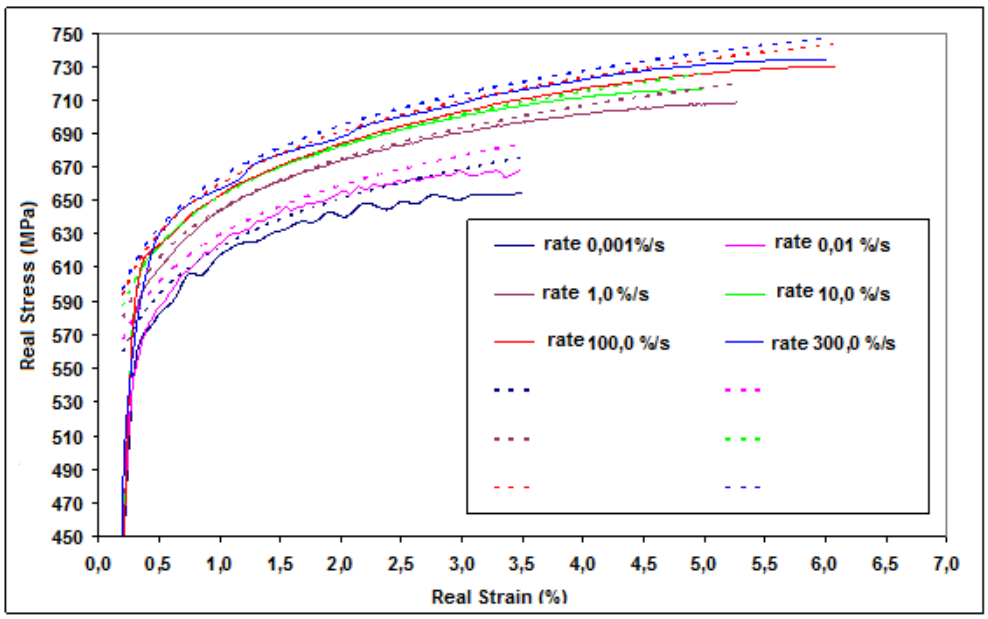

Figure 7: Set of Johnson-Cook by Levemberg-Marquardt at measured curves.

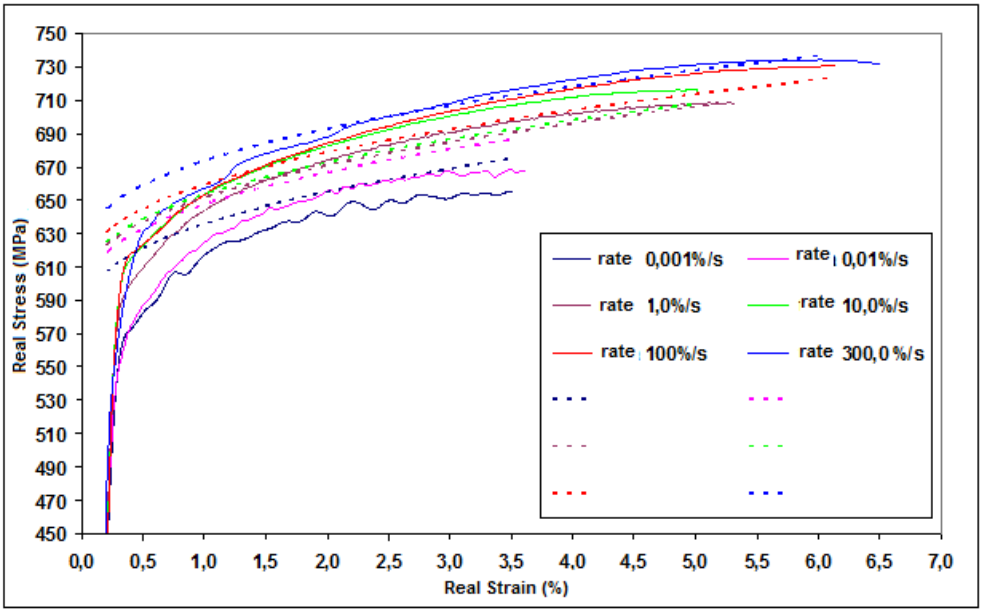

Figure 8: Set of Zerrili-Armstrong by Levemberg-Marquardt at measured curves.

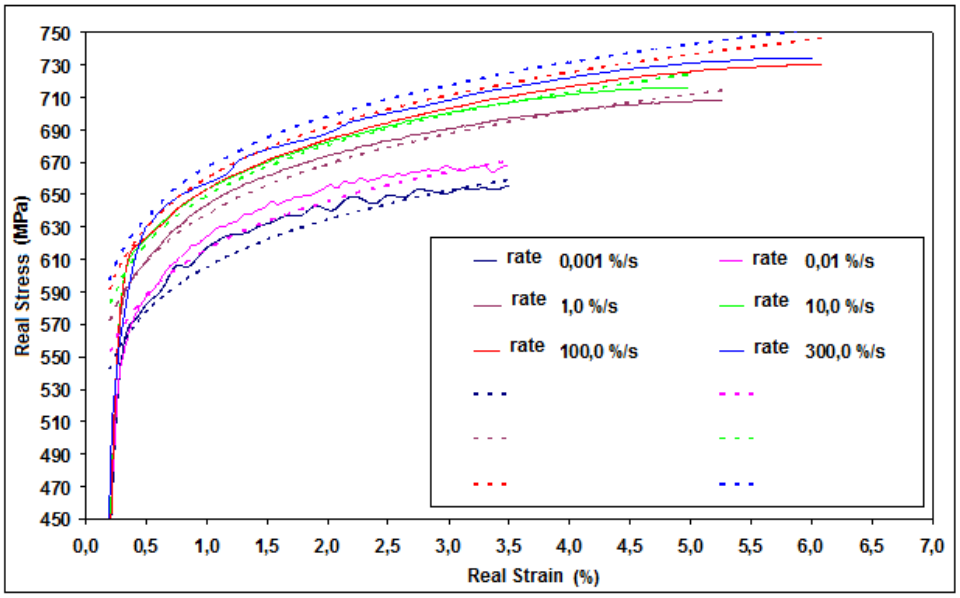

Figure 9 : Set of Johnson-Cook modified by Levemberg-Marquardt at measured curves.

The prediction of S_E and S_R as a function of strain rate (from strengths measured at reference rate $\dot{\varepsilon} = 0.25\% / s$) by Johnson-Cook is compared with data measured in Figs 10 and 11. Table 2 shows the correlation coefficient between the curves and measures provided by the various models studied here. Finally, Table 3 show parameters of the various models fitted by the LM curves **(σ×ε)** real.

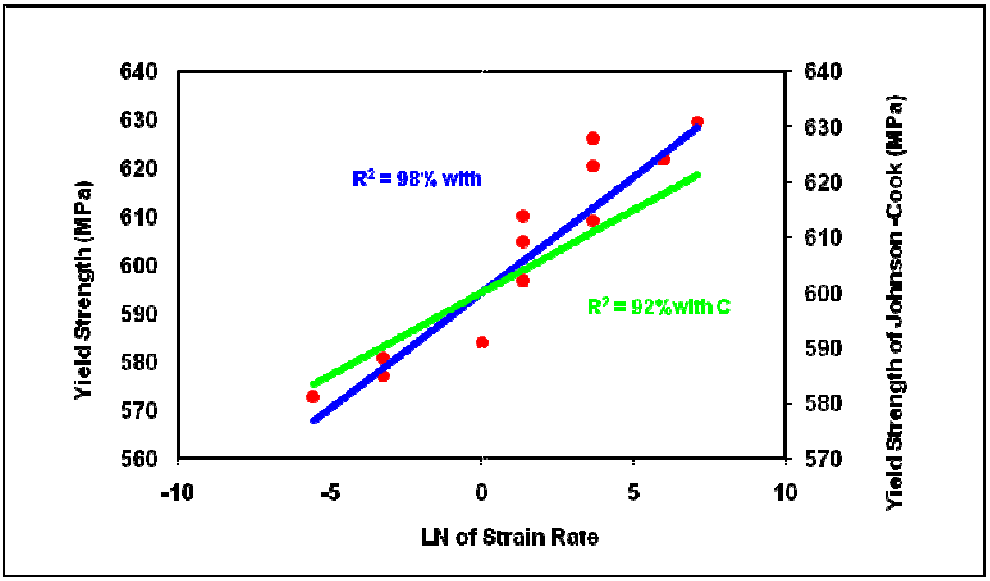

Figure 10: Comparing the yield strength measured with the yield strength provided by Johnson-Cook.

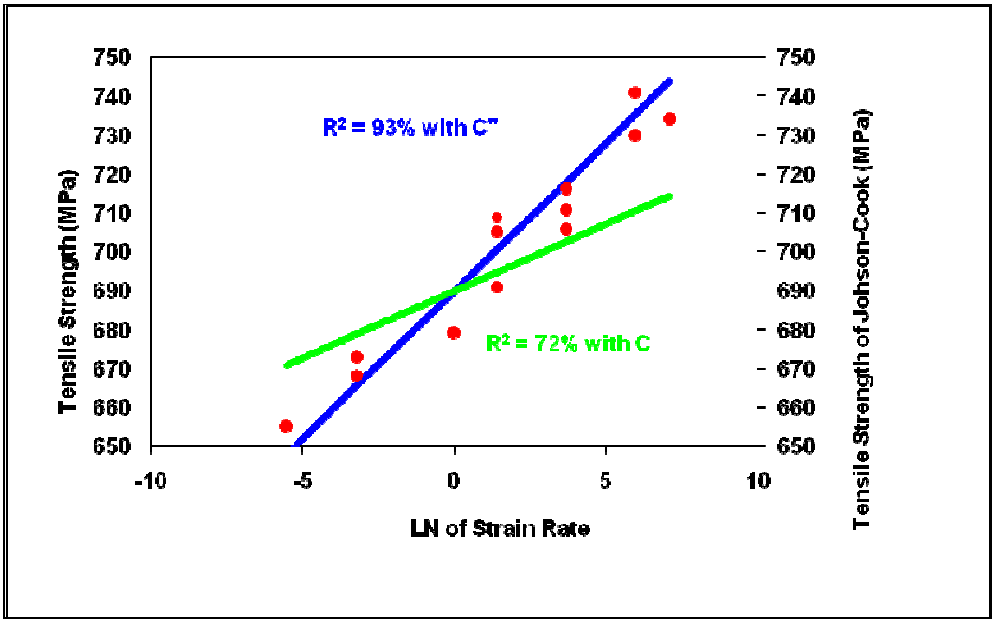

Figure 11: Comparing the tensile strength measured with the tensile strength provided by John-son-Cook.

The figure 10 shows the predictions using the generated S_E parameter C = 0.005 been obtained by fitting-Johnson-Cook LM can be improved by using C "= 0.007. An even more significant improvement occurs using C = 0.011" to predict S_R, in accordance with figure 11. Thus, these local adjustments can be useful in such tasks.

Strain Rate (%/s)	Johnson Cook R^2 (%)	Zerilli Armstrong modified R^2 (%)	Johnson Cook modified R^2 (%)
0,001	72,4	25,6	85,9
0,01	79,8	24,9	87,6
1,0	88,8	74,5	90,9
10	84,5	64,4	85,9
100,0	77,6	60,5	77,5
300,0	84,2	60,9	81,7
Média	81,2	51,8	84,8

Table 2. Correlation coefficient between the curves and the measures provided for by adjusting the various models through Levemberg-Marquardt algorithm

Parameters	Johnson Cook	Zerilli Armstrong modified	Johnson Cook modified
B	660 MPa	-	660 MPa
C	0,0050	-	0,0052
n	0,066	0,4	0,068
B_1	-	60 MPa	-
C_1	-	3,0 MPa	-

Table 3. Parameters resulting from the adjustment for the various models of LM curves σ×ε real measures

5 CONCLUSIONS

The influence of strain rate in stress x strain curves, yield strength and tensile strength of cold rolled 1020 steel was studied, through different dynamic tensile tests controlled by the strain rate, and not by the velocity v from piston of the servo-hydraulic machine. This procedure eliminate the systematic errors generated when mistakenly assume that $\dot{\varepsilon} = v/L$, where L is the length of the base measures the specimen, which may be substantial. The influence of the rate in the elastic phase is negligible, but, as expected, the strength increase at fast rates, and what is not intuitive, so does the ductility of the material tested. In the studied range, which includes strain rates $10^{-5} \leq \dot{\varepsilon} \leq 3\ s^{-1}$ covering a 5 ½ orders of magnitude, the semi-empirical model of Johnson-Cook describes reasonably variation of approximately 10% of the measured properties in higher rates lower and higher, but the best correlations are obtained by setting specific property or the desired behavior. Therefore, when it is necessary to make predictions using this model, one must take care to ensure the data were measured and the parameters of the model are adjusted to them.

REFERENCES

1 FROST, H.J.; ASHBY, M.F. Deformation Mechanisms Maps, Pergamon, 1982.

2 BACKOFEN, W.A. Deformation Processing, Addison-Wesley, 1972.

3 DIETER, G.E. Mechanical Metallurgy, McGraw Hill, 1976.

4 COTTRELL, A.H. The Mechanical Properties of Matter, Krieger, 1981.

5 LEMAITRE, J.; CHABOCHE, J.L. Mechanique des Matériaux Solides, Bordas, 1985.

6 THOMPSON, A.C. High Strain Rate Characterization of Advanced High Strength Steels. Waterloo, 2006.

7 ASM Handbook v. 8, Mechanical Testing and Evaluation, ASM, 2000.

8 CASTRO, J.T.P.; MEGGIOLARO, M.A. "Fadiga - Técnicas e Práticas de Dimensionamento Estrutural sob Cargas Reais de Serviço: Volume II - Propagação de Trincas, Efeitos Térmicos e Estocásticos", ISBN 1449514707, CreateSpace, 2009.